

# VALIDATION OF INTERMITTENCY MODEL FOR TRANSITION PREDICTION IN A RANS FLOW SOLVER

de Rosa Donato\* , Catalano Pietro\*

\*CIRA Italian Aerospace Research Center, Capua (CE), 81043, Italy

**Keywords:** RANS, Transition prediction, Intermittency model

## Abstract

*Turbulence models are widely accepted in CFD codes in order to close Reynolds Averaged Navier Stokes equations. In the years more and more complex models were proposed to improve the reliability of numerical results, anyway laminar and transition regions are neglected. A way to compute the upstream flow field as laminar is to impose a transition line. This technique requires that transition location is known a priori from experimental data or using other transition prediction approaches as  $e^N$  method. Nevertheless, transition region is not computed and a sudden shift between laminar and turbulent region is observed. In the last decades, several methods to model transition region in CFD codes have been investigated and following the last developments the authors decided to implement the  $\gamma$  model into in-house flow solver. Results of the implementation of the model are presented relative to 2D and 3D test cases and the introduced transition prediction capabilities are demonstrated.*

## 1 Introduction

The prediction of boundary-layer transition region plays a key role in the simulation of aerodynamic flows, especially for airfoil and wing design, to correctly predict lift and drag forces and, thus, the overall performance. This requirement is further stressed for all the cases where the laminar-turbulent transition process highly influences the flow-field, such as for natural laminar-flow, laminar flow control, rotor heli-

copter and wind turbine blade design. Reynolds Averaged Navier Stokes (RANS) equations are widely used by the aeronautical industry for the simulation of viscous flows. Important physical phenomena, such as boundary layer separation and shock-boundary layer interaction, largely affect the global flow parameters (e.g. drag coefficient), and can be predicted with sufficient accuracy only by a correct simulation of the whole flow field. CFD codes' capabilities in simulating fully turbulent flows have been widely assessed, as well as the coupling between RANS solver and transition prediction tools as described in[1]. Models to expressly simulate the transition phenomenon in a RANS environment are quite new. Some are based on a physics-based RANS model formulations and the most prominent is the Laminar Kinetic Energy proposed by Walters and Leylek[2, 3]. Recently, a new correction was also proposed by Lopez and Walters[4]. An alternative to physics-based formulation is the so-called Local-Correlation based Transition Modeling (LCTM) concept, where the different transition processes are not modeled, but a set of transport equations are formulated to combine experimental correlations via triggering functions. A widely known model is the one proposed by Langtry and Menter[5], namely the  $\gamma-Re_\theta$  model. In 2015, Menter et al.[6] proposed a new transition model, namely the  $\gamma$  model, that is based on the previous one but only one transport equation for the intermittency is present while the momentum-thickness Reynolds number is algebraically computed using local variables. This paper deals with the implementation of  $\gamma$  model,

coupled with the  $\kappa - \omega$  SST turbulence model, into in-house RANS flow solver UZEN[7] and its validation. The aim is to demonstrate the transition prediction capabilities of the newly introduced model in the solver.

## 2 Test case

The implementation of the transition model was validated on 2D and 3D flows. For bidimensional analyses, the model was tested on a zero pressure gradient flat plate and on a laminar-flow airfoil designed for horizontal-axis wind-turbine applications where laminar separation bubbles are present. A detailed description of validation phase was discussed in [8], while in this paper only the main results are reported. In order to perform further analyses on 2-D geometries, an additional test case, consisting of a two components airfoil, was considered. For this last case only a numerical comparison is available, due to lack of experimental data. Prolate spheroid was used as tridimensional test case. The results obtained are consistent with theoretical considerations and in good agreement with the available experimental data.

### 2.1 Flat plate

Two test cases from the ERCOFTAC T3 series[9] were considered to validate the implementation of the model in the code on flat plate geometry. The T3A and T3B setup were analyzed, respectively. Both tests are zero pressure gradient and freestream conditions are listed in table 1:

Table 1 Flat plate conditions		
	T3A	T3B
M	0.0152	0.0276
Re	$5.67 \times 10^5$	$1.03 \times 10^6$
Tu	3.30%	6.20%

A 2 blocks structured grid was generated on a rectangular domain  $\Omega = [-0.2, 1.6] \times [0, 0.3]$  where the flat plate starts at  $x = 0$ . Three different mesh sizes were considered, namely “Coarse”,

“Medium” and “Fine”, consisting of 5376, 21504 and 86016 cells, respectively.

The skin friction coefficient on T3A configuration, obtained on the three different grids, is compared with the experimental data in figure 1. It can be seen that the model manages to foresee transition onset on all the grids, and refining the mesh improves the match with experimental data.

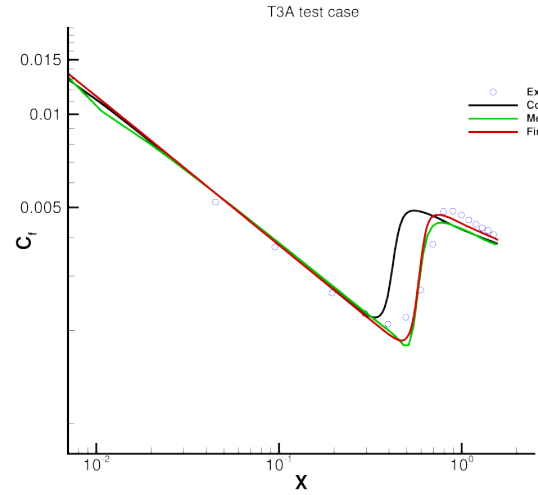


Fig. 1 T3A flat plate

Similar conclusions are obtained for T3B configuration as shown in figure 2.

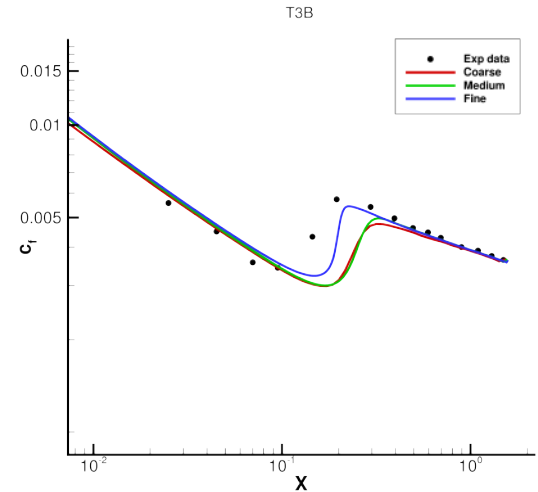


Fig. 2 T3B flat plate

## 2.2 S809 airfoil

The S809 is a 21%-thick, laminar-flow airfoil designed for horizontal-axis wind-turbine applications. It was designed and analyzed theoretically and verified experimentally in the low-turbulence wind tunnel of the Delft University of Technology Low Speed Laboratory[10]. The airfoil presents short laminar separation bubbles at high Reynolds number and is particularly challenging as these bubbles are not predicted in fully turbulent simulations[11].

Flow conditions for this test are  $M = 0.10$  and  $Re = 2.0 \times 10^6$ , while freestream turbulence is set as  $Tu = 0.05\%$ . The simulations range from  $\alpha = 1^\circ$  to  $\alpha = 9^\circ$ . A single block structured mesh with a C topology was used with three different grid refinements made of 38016, 67584 and 152064 cells, respectively.

The experimental/numerical comparison in terms of pressure coefficient is shown from figure 3 to figure 5 for three angles of attack.

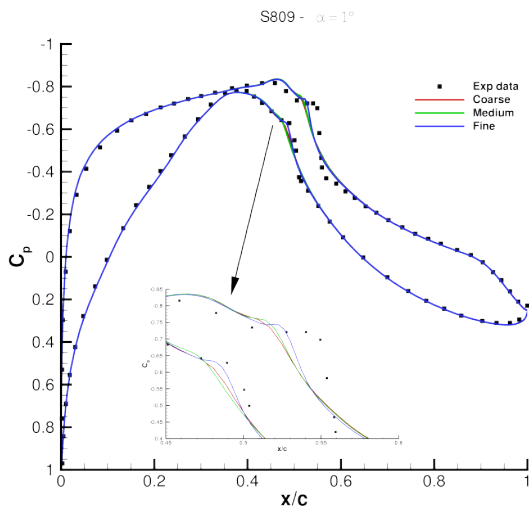


Fig. 3 S809 -  $C_p$  at  $\alpha = 1^\circ$

The match with experimental data is satisfactory for all the simulations, and the bubble location is well predicted while refining the grid. A comparison in terms of transition abscissa is also available and it is shown in figure 6.

It can be observed that the match is fairly good at all incidences on both upper and lower

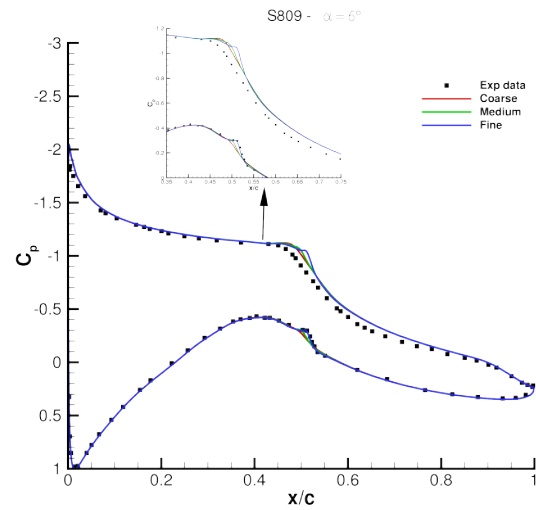


Fig. 4 S809 -  $C_p$  at  $\alpha = 6^\circ$

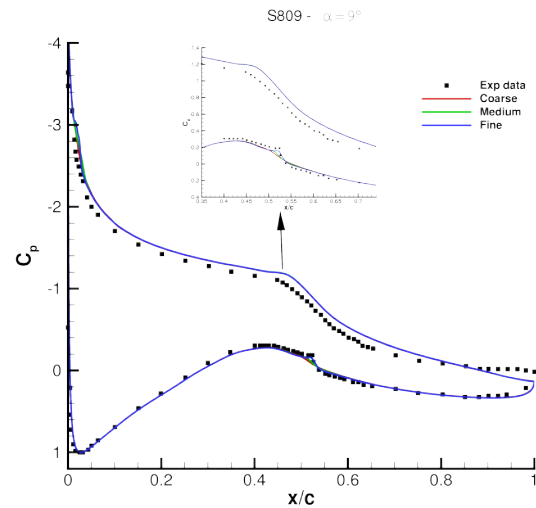
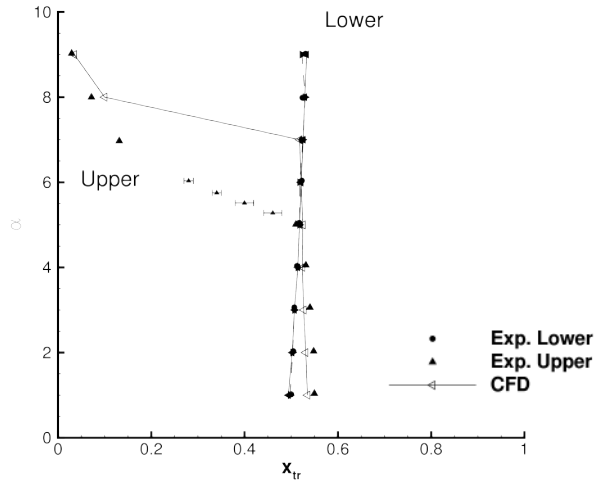


Fig. 5 S809 -  $C_p$  at  $\alpha = 9^\circ$

sides. It must be pointed out that on the upper side the experimental data show a sudden upstream shift of transition point in the range  $5^\circ \leq \alpha \leq 7^\circ$ . This effect is returned in numerical simulations, but it occurs with a delay of about one degree.

Drag polar and lift coefficient curves are shown in figures 7 and 8, respectively. Experimental data in free transition are compared with results obtained by fully turbulent and intermittency model simulations. Fully turbulent results foresee a higher drag coefficient than the experi-



**Fig. 6** S809 - transition abscissa

mental one, as expected. Data obtained by intermittency model allow for a large improvement of the  $C_d$  and show a shift in  $C_l$ .

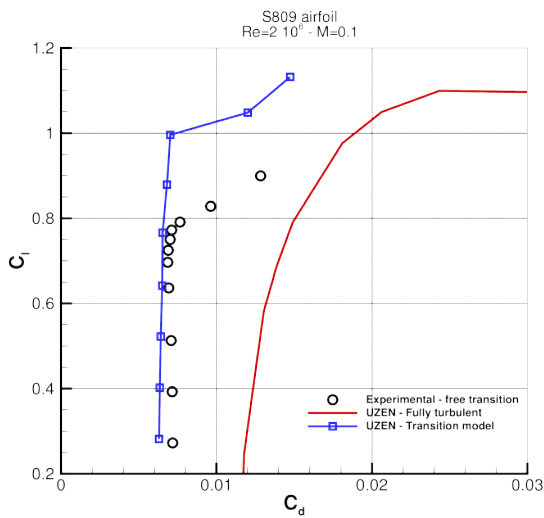


**Fig. 7**  $C_l - C_d$ , experimental - numerical comparison

### 2.3 High-lift airfoil

The transition model has been also applied to a two-components airfoil, (figure 9) in high-lift conditions. The specification of the flow is  $M = 0.2$  and  $Re = 4.65 \times 10^6$ . Different angles of attack have been considered.

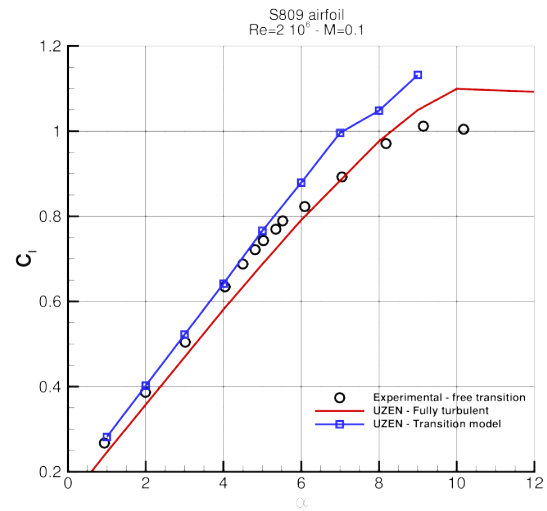


**Fig. 8** Lift coefficient curve, experimental - numerical comparison



**Fig. 9** Bi-component airfoil

The plan is to perform simulations with "fully turbulent" assumption and also by fixing the transition points. The procedure usually employed to detect the transition points is to perform a preliminary computation by the MSES code[12] in free transition. Then, the transition locations returned by MSES are used as input by the UZEN code. The  $\gamma$  model has allowed to perform also "free-transition" simulations.

For this test case, experimental data are not available yet, and only a numerical comparison is performed. The results obtained with the  $\gamma$  model are compared with RANS fully turbulent computations and with MSES code using 7 as critical  $N$  factor.

A comparison of the results achieved at  $\alpha = 5^\circ$  are shown, in terms of pressure and friction coefficients, in figure 10. The transition affects the friction distribution, while no large differences can be seen in the pressure coefficient. On the main component, MSES returns the transition very close to the leading edge of the upper sur-

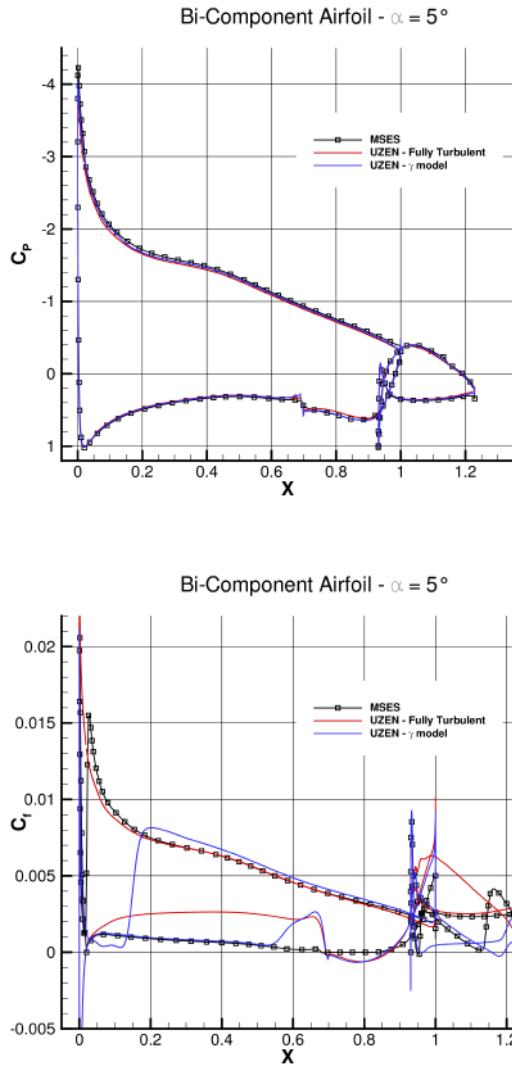


**Fig. 10** Bi-component airfoil,  $M = 0.20$ ,  $Re = 4.65 \times 10^6$  and  $\alpha = 5^\circ$ ,  $C_p$  (top) and  $C_f$  (bottom): – MSES

face and at the beginning of the recirculation region of the cove on the lower surface. Instead, the intermittency model provides a transition starting at about  $x = 0.12$  on the upper and at about  $x = 0.55$  on the lower surface. These differences in the transition detection impact the skin friction coefficient as it is particularly evident on the lower surface of the main. The friction coefficients recover the "fully turbulent" simulation in the turbulent part.

On the upper surface of the flap, the  $\gamma$  model follows the MSES solution with a transition located more downstream and a short bubble. Both

solutions being very different from the "fully turbulent" result. On the lower surface of the flap, MSES recovers the "fully turbulent" data while  $\gamma$  provides a more laminar  $C_f$ .

As  $\alpha$  increases, on the main component the intermittency model shifts the transition point upstream on the upper surface and downstream towards the cove on the lower surface. Both MSES and  $\gamma$  return a very tiny bubble in the leading edge region. This can be noted in the figures 11 and 12

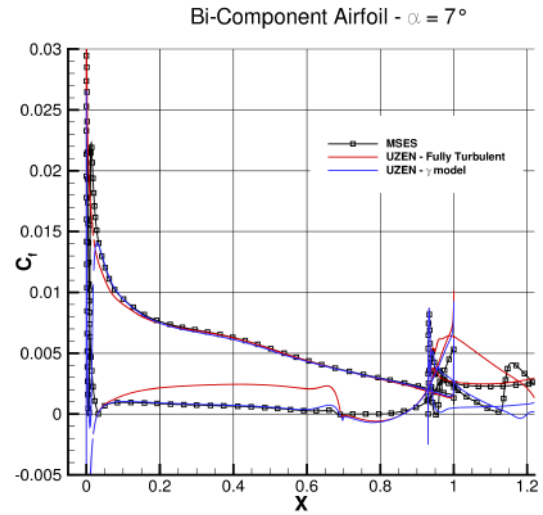


**Fig. 11** Bi-component airfoil,  $M = 0.20$ ,  $Re = 4.65 \times 10^6$  and  $\alpha = 7^\circ$

that report the  $C_f$  achieved at  $\alpha = 7^\circ$  and  $9^\circ$  respectively.

The friction coefficient on the flap at  $\alpha = 7^\circ$  and  $9^\circ$  resembles the distribution obtained at  $\alpha = 5^\circ$ . The only difference is that the bubble presented by the  $\gamma$  model enlarges with the incidence.

The  $\gamma$  model has allowed to perform "free-transition" simulations providing an alternative to the approach based on the MSES code and on the evaluation of the transition points through the  $N$  factor method.

The results are congruent with the "fully turbulent" simulation and have shown some differences. In particular on the lower surface of the main component, MSES provides the transition where the flows starts to separate in the cove region. The  $\gamma$  model, instead, gives an increase of



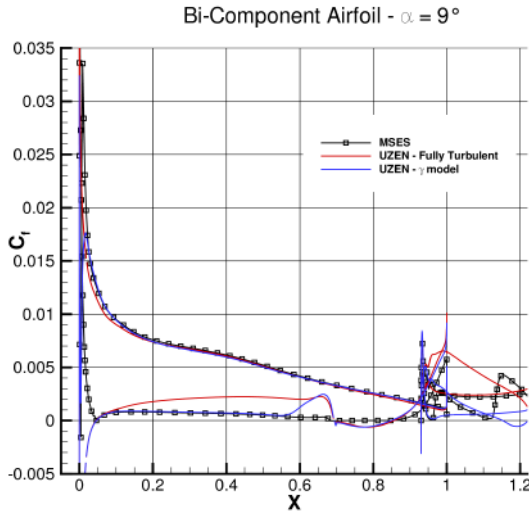


**Fig. 12** Bi-component airfoil,  $M = 0.20$ ,  $Re = 4.65 \times 10^6$  and  $\alpha = 9^\circ$

the  $C_f$  upstream the cove. Likely this should be due to a "by-pass" transition because only a weak compression is present in the pressure distribution. However the dependence of  $\gamma$  on the free-stream turbulence could have an effect and this should be investigated in more detail. On the flap, a bubble on the upper surface is obtained only by  $\gamma$ , and this could affect the stall characteristics of the airfoil.

## 2.4 Prolate spheroid

The 6:1 inclined prolate spheroid is a three-dimensional configuration widely used for testing transition prediction methods. The experiments were conducted in the low-speed tunnel at DLR by Kreplin et al.[13]. For such configuration transition occurs both for Tollmien-Schlichting and crossflow instabilities. On this side, several extensions for crossflow instabilities were proposed for the  $\gamma - Re_\theta$  model[14, 15, 16, 17], yielding reasonable results. However, the present model is implemented without crossflow correlations, so results diverging from the experimental data are expected. Two different cases were taken into account, the first with a  $Re = 6.50 \times 10^6$  (Case 1) and the second with a  $Re = 1.50 \times 10^6$  (Case 2). For Case 1, three different angles of attack were considered  $\alpha = 5^\circ$ ,  $10^\circ$  and  $15^\circ$ , while for

Case 2 only  $\alpha = 10^\circ$  was simulated. Freestream turbulence and eddy viscosity ratio are set as  $Tu = 0.15\%$  and  $\mu_t/\mu = 0.10$ , respectively. All simulations were performed on a structured grid made of 16 blocks and approximatively  $8 \times 10^6$  cells.

Comparison with experimental data is made on skin friction distribution. Figures 13, 14 and 15 refer to Case 1 at  $\alpha = 5^\circ$ ,  $10^\circ$  and  $15^\circ$ , respectively. Top side of figures reports experimental data while bottom side shows numerical results. Both real and unwrapped spheroid surfaces are depicted.

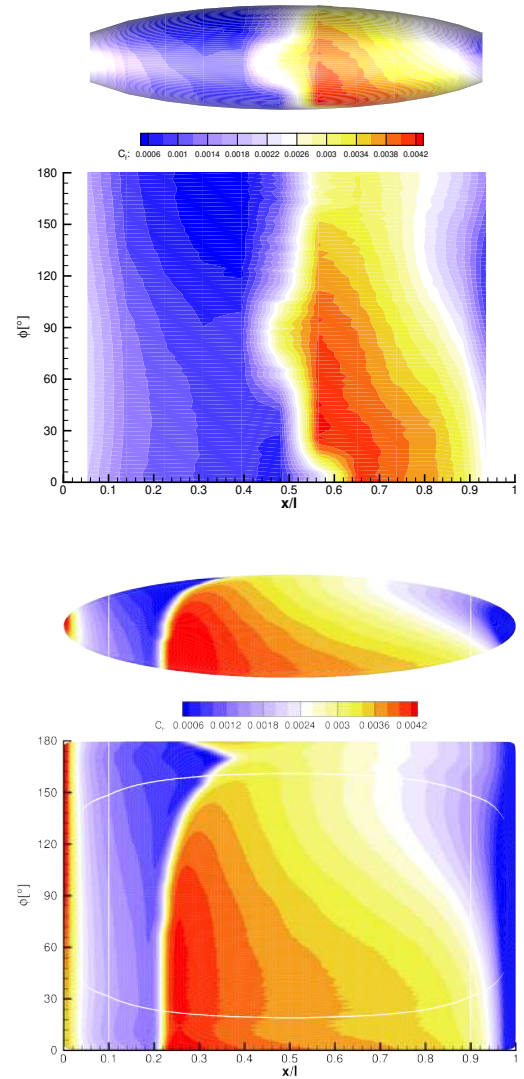


**Fig. 13** Spheroid,  $Re = 6.5 \times 10^6$  and  $\alpha = 5^\circ$ ,  $c_f$  distribution (top: experimental; bottom: simulated)

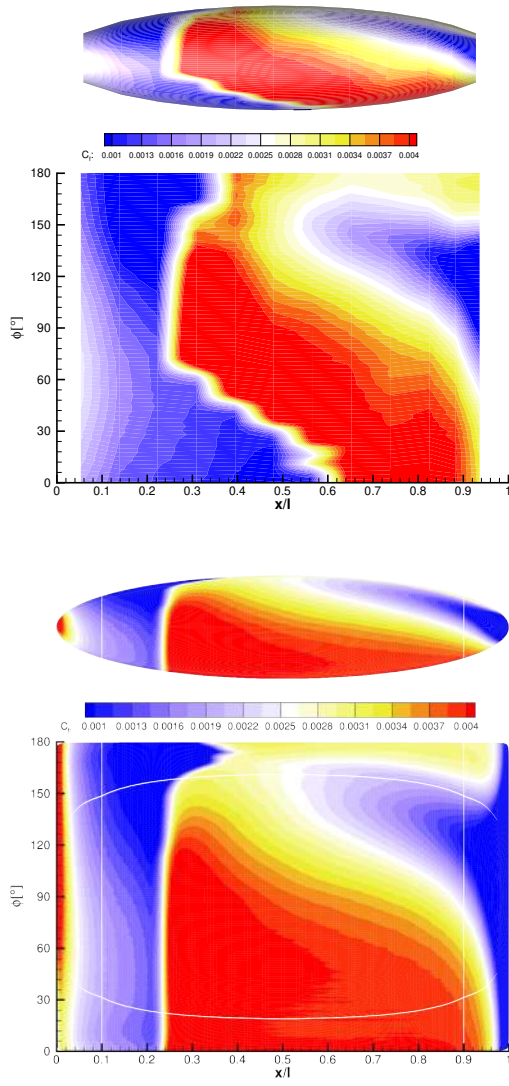


**Fig. 14** Spheroid,  $Re = 6.5 \times 10^6$  and  $\alpha = 10^\circ$ ,  $c_f$  distribution (top: experimental; bottom: simulated)

For all the inclinations, a good agreement with experiments is found on the leeward side. At  $\alpha = 5^\circ$ , transition onset is predicted too far upstream, resulting in a more extended turbulent region. At  $\alpha = 10^\circ$  and  $\alpha = 15^\circ$ , the increase of skin friction occurs numerically at constant abscissa, while experiments show a transition line in the range  $0^\circ \leq \phi \leq 60^\circ$ .

For Case 2, result is shown at  $\alpha = 10^\circ$  in figure 16. The trend in skin friction distribution is well predicted on the whole geometry, even though a wider extension of “high” skin friction values is observed on the windward side in the

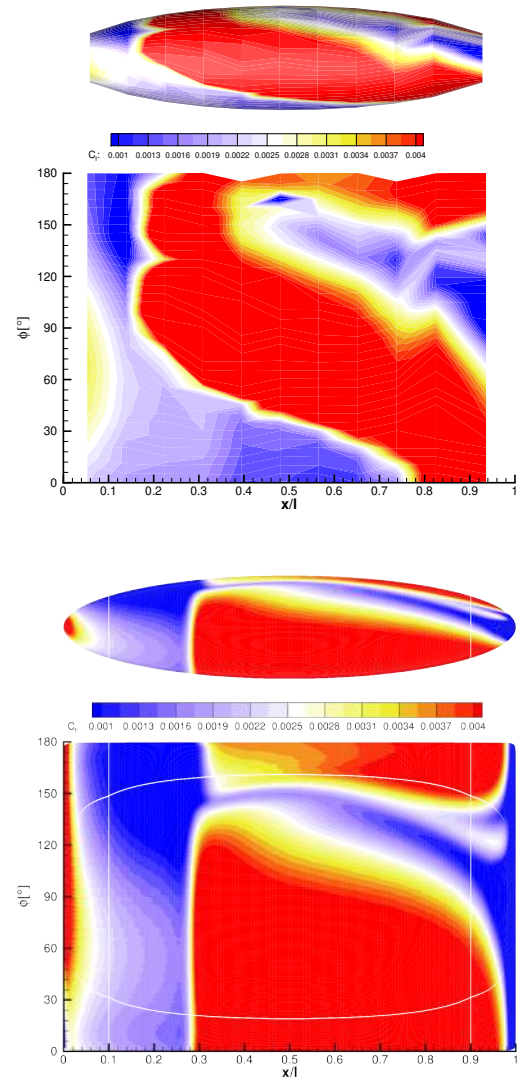


**Fig. 15** Spheroid,  $Re = 6.5 \times 10^6$  and  $\alpha = 15^\circ$ ,  $c_f$  distribution (top: experimental; bottom: simulated)

numerical simulation.

Despite the model was used without specific correlation for CF instabilities, results show a good qualitative and quantitative match with reference to experimental data.

### 3 Conclusions

The local correlation-based  $\gamma$  transition model for the prediction of laminar-turbulent transition, coupled with the  $\kappa - \omega$  SST turbulence model, was implemented in the in-house CFD structured code.

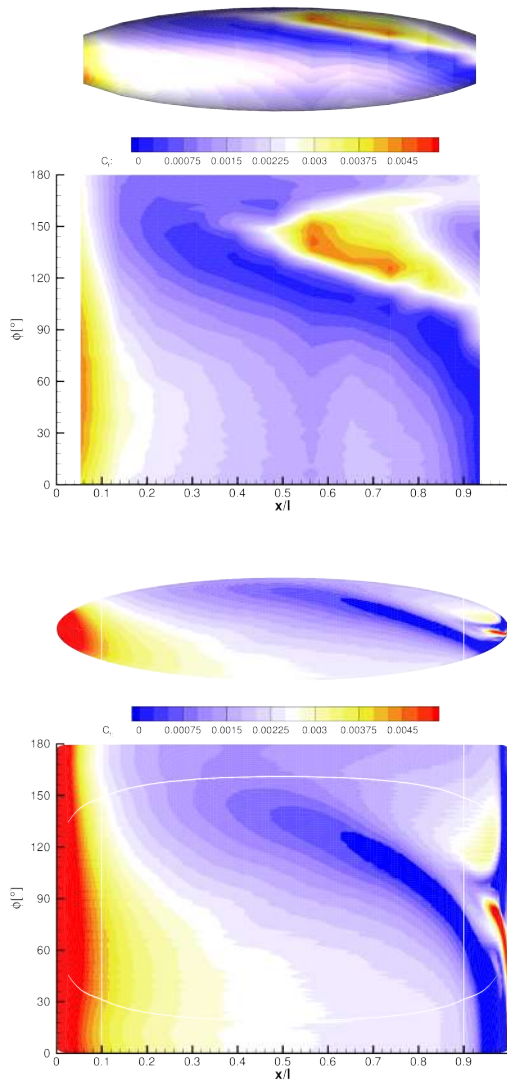


**Fig. 16** Spheroid,  $Re = 1.5 \times 10^6$  and  $\alpha = 10^\circ$ ,  $c_f$  distribution (top: experimental; bottom: simulated)

A preliminary validation of the newly introduced model was performed on a zero pressure gradient flat plate. The ERCOFTAC T3A and T3B test cases were taken into account, providing satisfactory results.

For bi-dimensional application, two different airfoils were considered. The first one was the S809 airfoil, whose main characteristic is the presence of laminar separation bubbles, resulting in a challenging test case for turbulence models. The results on S809 airfoil clearly showed the improvement of the transition model with respect to a fully turbulent approach. Nevertheless, more

detailed analyses are required to improve the prediction of transition abscissa at critical angles of attack, i.e.  $\alpha \approx 6^\circ$ .

The second 2-D test case is a bi-component airfoil in landing conditions. Flow-field computed with transition model presents characteristics not returned by the fully turbulent simulations. Differences, especially on the flap, are shown also with reference to “fixed” transition approach based on  $N$  method. Anyway experimental data are necessary to confirm the results.

The 6:1 inclined prolate spheroid was used as three-dimensional test case. Despite the lack of a crossflow extension, results showed a reasonable agreement, within the limit of the model itself. For all simulations a good agreement was found on the leeward side of the spheroid, while on the windward side discrepancies with the experiments are present.

## References

- [1] Raffaele S. Donelli and Donato de Rosa. Stability analysis of three-dimensional laminar compressible boundary layers based in ray-tracing theory and multiple scale technique. *Aerotecnica Missili & Spazio*, 95(4), Dec 2016.
- [2] D. Keith Walters and James H. Leylek. A new model for boundary layer transition using a single-point rans approach. *Journal of Turbomachinery*, 126(1):193–202, Mar 2004.
- [3] D. Keith Walters and James H. Leylek. Computational fluid dynamics study of wake-induced transition on a compressor-like flat plate. *Journal of Turbomachinery*, 127(1):52–63, Feb 2005.
- [4] Maurin Lopez and D. Keith Walters. A recommended correction to the  $k_t - k_l - \omega$  transition-sensitive eddy-viscosity model. *Journal of Fluids Engineering*, 139(2):024501, dec 2016.
- [5] Robin Langtry and Florian Menter. Transition modeling for general CFD applications in aeronautics. In *43rd AIAA Aerospace Sciences Meeting and Exhibit*. American Institute of Aeronautics and Astronautics (AIAA), jan 2005.
- [6] Florian R. Menter, Pavel E. Smirnov, Tao Liu, and Ravikanth Avancha. A one-equation local



correlation-based transition model. *Flow, Turbulence and Combustion*, 95(4):583–619, 2015.

- [7] Pietro Catalano and Marcello Amato. An evaluation of RANS turbulence modelling for aerodynamic applications. *Aerospace Science and Technology*, 7(7):493–509, oct 2003.
- [8] Donato de Rosa and Pietro Catalano. Validation of intermittency model for transition prediction in a rans flow solver. In *2018 AIAA Aerospace Sciences Meeting*, page 1043, 2018.
- [9] [http://cfd.mace.manchester.ac.uk/ercoftac/database/cases/case20/Case\\_data/](http://cfd.mace.manchester.ac.uk/ercoftac/database/cases/case20/Case_data/).
- [10] D M Somers. Design and experimental results for the s809 airfoil. Technical report, jan 1997.
- [11] Pietro Catalano, Renato Tognaccini, and Benedetto Mele. A numerical method to detect laminar separation bubbles over airfoils. In *31st AIAA Applied Aerodynamics Conference*. American Institute of Aeronautics and Astronautics, jun 2013.
- [12] Mark Drela. *A User's Guide to MSES 2.9*. MIT Computational Aerospace Sciences Laboratory, October 1995.
- [13] H.-P. Kreplin, H. Meier, and A. Maier. Wind tunnel model and measuring techniques for the investigation of three-dimensional turbulent boundary layers, 1978.
- [14] Cornelia Seyfert and Andreas Krumbein. Correlation-based transition transport modeling for three-dimensional aerodynamic configurations, 2012.
- [15] Shivaji Medida and James Baeder. A new cross-flow transition onset criterion for rans turbulence models, 2013.
- [16] Cornelia Grabe and Andreas Krumbein. Extension of the  $\gamma - re_{\theta}$  model for prediction of cross-flow transition. In *52nd Aerospace Sciences Meeting*. American Institute of Aeronautics and Astronautics (AIAA), jan 2014.
- [17] Cornelia Grabe, Nie Shengyang, and Andreas Krumbein. Transition transport modeling for the prediction of crossflow transition, 2016.

## Copyright Statement

The authors confirm that they, and/or their company or organization, hold copyright on all of the original material included in this paper. The authors also confirm that they have obtained permission, from the copyright holder of any third party material included in this paper, to publish it as part of their paper. The authors confirm that they give permission, or have obtained permission from the copyright holder of this paper, for the publication and distribution of this paper as part of the ICAS proceedings or as individual off-prints from the proceedings.

## 4 Contact Author Email Address

mailto: d.derosa@cira.it